Am J Transl Res 2021;13(12):13608-13624
www.ajtr.org /ISSN:1943-8141/AJTR0122739

Original Article

Preclinical model-based evaluation of Imatinib resistance induced by *KIT* mutations and its overcoming strategies in gastrointestinal stromal tumor (GIST)

Qian Zhao[1], Cheng Zhang[1], Changsong Qi[1], Jing Yang[1], Yang Chen[1], Sai Ge[1], Lin Shen[1], Jing Gao[2], Jian Li[1]

[1]*Department of Gastrointestinal Oncology, Key Laboratory of Carcinogenesis and Translational Research (Ministry of Education/Beijing), Peking University Cancer Hospital & Institute, 52 Fucheng Road, Beijing 100142, China;* [2]*National Cancer Center/National Clinical Research Center for Cancer/Cancer Hospital & Shenzhen Hospital, Chinese Academy of Medical Sciences and Peking Union Medical College, Shenzhen 518000, Guangdong, China*

Received September 20, 2020; Accepted October 12, 2021; Epub December 15, 2021; Published December 30, 2021

Abstract: Background: The potential correlation between *KIT* secondary mutations and Imatinib-resistance in gastrointestinal stromal tumor (GIST) has been hinted, yet their specific linkage and underlying mechanisms remained unelucidated, also the development of substitute strategies dealing with this resistance was urgently needed. Methods: In this study, we explored the distribution of the most prevalent forms of *KIT* mutation in Chinese GIST patients, after that, we established cell lines that was overexpressed with mutant KIT, and by performing RNA sequencing, immunoblotting and cell viability, we analyzed their functional and mechanistic relevance with Imatinib-resistance in GIST cell lines. Additionally, we evaluated the tumor inhibition efficacy of four regimens in Imatinib-resistant GIST cell lines and patient-derived xenograft (PDX) models. Results: We found that *KIT* exon 13-V654A and exon 17-N822K were the most common secondary mutations in GIST with primary exon 11 mutations. These two secondary mutations induced Imatinib resistance by activating PI3K-Akt signaling pathway, while PI3K-Akt inhibition rescued the resistance. By assessing the feasibility of other four tyrosine kinase inhibitor (TKIs, Sunitinib/Regorafenib/Avapritinib/Ripretinib) against Imatinib-resistant GIST, we found that Sunitinib was more suitable for *KIT* exon 13 secondary mutations, the rest were more effective for *KIT* exon 17 secondary mutations, while all four TKIs displayed efficacy for *KIT* exon 9 mutations, emphasizing their clinical applications against Imatinib resistance. Conclusions: We demonstrated the mechanism by which *KIT* secondary mutations on exon 13/17 cause Imatinib resistance to GIST, and validated that several novel TKIs were valuable therapeutic options against Imatinib-resistance for both secondary- and primary-*KIT* mutations.

Keywords: Gastrointestinal stromal tumor, *KIT* mutations, imatinib resistance, preclinical-therapeutic evaluation, avapritinib, ripretinib

Introduction

Gastrointestinal stromal tumor (GIST), the most common alimentary canal interstitial tumor, was considered to be originated from the mesenchymal cells of Cajal (the pacemaker cells of the gastrointestinal tract) or related stem cells [1, 2]. The prevalence of GIST continues to increase, with approximately 5,000 new cases each year. While GISTs can arise anywhere from esophagus to rectum, the majority originate from the stomach (60-70%) and small bowel (20-30%) [3]. Traditionally, surgery was the only approach of radical cure for GIST with a 5-year survival rate of 48-54% [4], while patients with irresectable or metastatic disease survived only for a median of 18-24 months after diagnosis with a 5-year survival rate of 5-10% [5, 6].

GISTs are driven and characterized by *C-Kit* (*KIT*) or platelet-derived growth factor receptor alpha (*PDGFRA*) activating mutations, which approximately account for 80% or 10% of GIST patients, respectively [7]. With the development of targeted therapies, Imatinib mesylate, a selective inhibitor against mutant forms of type II tyrosine kinases, such as *KIT*, *PDGFRA*

and *ABL*, has been used as a paragon of first-line treatment for patients with advanced GIST, which dramatically improved the 5-year survival and recurrence rate [8-11]. However, most patients with initial clinical benefit from Imatinib eventually progress, typically within 29 months [12, 13]. Therefore, it is necessary to uncover the underlying molecular mechanisms of acquired resistance to Imatinib so as to further improve the survival of GIST patients.

Mainly observed on the ATP-binding pocket encoded by exon 13 and 14 and the activation loop encoded by exon 17 and 18, secondary mutations of *KIT* gene were found after Imatinib failure in up to 90% of GIST patients. Thus, tumor subclones carrying heterogeneous secondary *KIT* mutations were considered to reactivate *KIT* downstream signaling and continuously drive GIST proliferation and survival [14-17]. However, the molecular correlation between *KIT* mutations and Imatinib resistance, as well as the underlying mechanisms were still uncertain. In order to develop substitute regimens after Imatinib resistance, the applicable drug spectrum for GIST with different *KIT* mutations also remained to be established.

In our study, we analyzed 2273 Chinese GIST patients to identify the mutational spectrum of *KIT* mutations. By applying cell lines and PDX models, we evaluated the impact and underlying mechanisms of the most representative types of secondary *KIT* mutations on Imatinib sensitivity, and compared the anti-GIST efficacy of four candidate TKIs (Sunitinib, Regorafenib, Avapritinib and Ripretinib) to replace Imatinib for specific *KIT* mutations.

Materials and methods

Origination of patients and clinical information

Patients' specimens for *KIT* mutations assessment and xenograft construction were collected with the assistance of the gastrointestinal surgery by the Department of Pathology and Department of Gastrointestinal Oncology, Peking University Cancer Hospital & Institute. The diagnosis of GIST and *KIT* mutational spectrum were confirmed by histological analysis or Sanger sequencing for all cases. The experimental applications of patient samples and information (including basic parameters, therapeutic responses and medical images) have been approved by the Institutional Ethics Committee, Peking University Cancer Hospital & Institute and performed in accordance with the Declaration of Helsinki Principles. Written informed consents were obtained from all providers.

Clinical information of all patients was recorded and followed up by Department of Gastrointestinal Oncology, Peking University Cancer Hospital & Institute. Responses of patients were defined based on the Response Evaluation Criteria in Solid Tumors (RECIST 1.1). The progression-free survival (PFS) was calculated respectively, which started from the treatment of Imatinib and ended with progressive disease or death for any cause.

Cell culture, virus transfection and Imatinib-resistance induction

GIST-T1 and GIST-882 are human GIST cell lines with a *KIT* exon 11 heterozygous 560_578 deletion mutation and a primary *KIT* exon 13 homozygous K642E missense mutation, respectively [18, 19]. Both cell lines were gifts from Dr. Wang (Changzheng Hospital, Shanghai, China), and has been maintained and used in our laboratory. Under 37°C, 5% CO_2 and appropriate humidity, GIST cells were cultured with Iscove, Modified Dulbecco Medium (Gibco, USA) supplemented with 20% fetal bovine serum (Gibco, USA) and 1% penicillin-streptomycin (HyClone, USA).

KIT cDNA clones carrying exon 13-V654A or exon 17-N822K were constructed with pLenti-EF1a-EGFP-F2A-Puro-CMV (Clontech), and were integrated into lentiviral particles by using a Transfect lentiviral packaging reagent (OBIO, Shanghai, China). GIST-T1 and GIST-882 were transfected with lentiviral particles containing vector, *KIT*/V654A or *KIT*/N822K plasmids, respectively, then administrated with puromycin (0.5-1 μg/mL, Gibco, USA) to select cell clones expressing KIT.

GIST-T1R and GIST-882R sub-cell lines were cultured by continuously culturing the progenitor cell lines with low-dose (16 nM) to high-dose (400 nM) Imatinib for 6 months.

Cell viability assay

GIST cells in the logarithmic growth phase were evenly planted in 96-well plates with 1×10^4 cells per well. After 24 hours, the culture medi-

um was replaced with fresh medium containing drugs (Imatinib/BEZ235/Sunitinib/Regorafenib/Avapritinib/Ripretinib) and cultured at 37°C for another 72 hours. Imatinib mesylate, Sunitinib, Regorafenib, Avapritinib, and Ripretinib were purchased from MedChemExpress. BEZ235 was purchased from Selleck.

The cell culture medium was then discarded and replaced by fresh medium containing 10% cell counting kit-8 (CCK-8, DOJINDO, Japan), and cultured under 37°C for 2-3 hours. The absorbance at 450 nm was measured with a microplate reader (Infinite F50, TECAN, Switzerland) and used to calculated cell viability. All the above experiments were repeated for at least three times.

Establishment of patient-derived xenografts

Tumor specimens from patients were first placed in fresh RPMI 1640 medium, cut into a 3-mm square-fragments and washed 3 times with RPMI 1640. The tumor samples (P0) were then stuffed into 18-gauge needles and planted subcutaneously into 6-8 weeks NOD/SCID mice (Huafukang Biotechnology Co., Ltd., Beijing, China). Tumor growth and body weight were measured twice a week. When the volume of xenograft tumor reached 750-1000 mm^3, the mice were sacrificed and the subcutaneous tumors (P1) were stripped, and then re-implanted into NOD/SCID mice according to the previous steps, sequentially establishing P2 and P3 passages of PDX. All procedures were performed in Peking University Cancer Hospital animal rooms under sterile conditions in accordance with the Guidelines for the Care and Use of Laboratory Animals of National Institutes of Health. This experiment was approved by the Ethics Committee of Peking University Cancer Hospital.

In vivo drug sensitivity assay

For established GIST PDX models, when xenograft tumors reached 150-250 mm^3, mice were randomly divided into control and experimental groups (5 mice for each group). The control group was given saline and the treatment group was given different drugs by gavage. The drugs and doses in the treatment groups were as follows: Imatinib 50 mg/kg twice a day, Sunitinib 40 mg/kg daily, Regorafenib 30 mg/kg daily, Avapritinib 30 mg/kg daily, Ripretinib 30 mg/kg daily. Mice were treated for 3-4 weeks and measured for tumor size and body weight every two days. Tumor volume was calculated using the following formula: volume = (length × $width^2$)/2. Tumor growth inhibition (TGI) rate was calculated using the following formula: TGI = 1-ΔT/ΔC×100% (ΔT = tumor volume changes of the drug treated group, ΔC = tumor volume changes of the control group on the final day of the study).

RNA/DNA extraction and sequencing

Total RNA was collected from specimens using Trizol method. Quality control was performed to ensure RNA integrity using an Agilent 2100 Bioanalyzer (Agilent Technologies, USA). RNA sequencing was performed by Novogene (Beijing, China) using an Illumina HiSeq instrument (Illumina, San Diego, CA, USA). Genomic DNA was collected by using QIAamp DNA Mini Kit (Qiagen, Hilden, Germany), and was testified by Next generation sequencing (NGS) with an Illumina HiSeq 2000 system (Illumina, San Diego, CA, USA). Expressional and genomic alterations were enriched by referring to the Kyoto Encyclopedia of Genes and Genomes (KEGG, https://www.kegg.jp/) and the Database for Annotation, Visualization, and Integrated Discovery Bioinformatics Resources (DAVID, http://david.abcc.ncifcrf.gov). These procedures were similar to our previous reports [20, 21].

Immunoblotting

Total proteins from cells or tissue were extracted with CytoBuster protein extraction reagent (EMD Millipore, USA) supplemented with protease inhibitors and phosphatase inhibitors (Roche, Germany). BCA method (Applygen, Beijing, China) was used to measure protein concentration. 30 μg proteins of each sample were electrophoresed by 10% SDS-PAGE and transferred to the Immobilon®-PSQ Membrane (Merck Millipore, Germany). The membrane was blocked with 5% albumin bovine V (Biotopped, Beijing, China) solution and incubated with primary and secondary antibodies under proper concentrations. Primary antibodies for phospho-KIT Y719 (#3319), KIT (#3074), phospho-AKT S473 (#4060), AKT (#4691), phosphor-S6 S240/S244 (#4858) and S6 (#2217), anti-rabbit IgG, HRP-linked antibody (#7074), anti-mouse IgG, and HRP-linked anti-

body (#7076) were from Cell Signaling Technology (Danvers, MA, USA), while antibody for β-actin was purchased from Sigma-Aldrich (St. Louis, Missouri, USA). The protein blots were illuminated with HRP substrate luminol reagent (Millipore, USA) and visualized using an Amersham Imager 600 (GE Healthcare, UK).

Immunohistochemistry and hematoxylin-eosin staining

PDX tumor tissues were fixed in formalin, embedded in paraffin, and then sliced into tissue sections. The tissue sections were subjected to deparaffinization, hydration, endogenous peroxidase treatment, and antigen retrieval steps, and then incubated with primary antibodies, IgG-HRP polymer (ZSJQB, Beijing, China) and diaminobenzidine substrate. To evaluate the histological characteristics of GIST, the tissue sections were stained with hematoxylin and eosin. Two pathologists from the Peking University Cancer Hospital's pathology department who were blinded to this study interpreted the sections.

Statistical analysis

Unpaired t test was used to analyze differences in cell viability between different groups. ANOVA was used to compare tumor growth among different groups with $P<0.05$ as statistically significant. The connection between *KIT* mutations and Imatinib treatment response were analyzed using Fisher's exact test. Log-rank test and Kaplan-Meier curve were used to analyze the correlation between the *KIT* mutation and PFS. Statistical analysis was performed with SPSS 20.0 software, and formatted with Graphpad Prism 6 software. For all analysis, $P<0.05$ was considered statistically significant.

Results

Specific mutations of KIT contributed to GIST's acquired resistance to Imatinib

We recruited 2273 Chinese GIST patients and assessed the clinicopathological characteristics of *KIT* mutations for validation (Supplementary Table 1). Among these patients, 3.0% (69) had wild-type *KIT* and wild-type *PDGFRA,* 4.8% (109) had mutated *PDGFRA*, while *KIT* and *PDGFRA* dual mutations were not observed. 92.2% (2095) patients harbored primary *KIT* mutations, in which exon 11-mutation (77.8%, 1769) was the dominant type, while mutations on exon 9 (11.5%, 263), exon 13 (1.5%, 33), and exon 17 (1.3%, 30) were also detected (**Figure 1A**). In these GIST patients, 130 received Imatinib therapy and developed resistance to Imatinib. Secondary mutations were detected in 38.5% (50) of them, including exon 13 (14.6%, 19), exon 17 (17.7%, 23), exon 14 (2.3%, 3) and exon 18 (3.9%, 5) (**Figure 1B**).

Patients harboring primary *KIT* exon 11 mutation displayed the best, while patients harboring primary *KIT* exon 9 mutation displayed the worst ORR (overall response rate) and PFS (progression-free survival) to Imatinib, thus they were considered as Imatinib-sensitive and Imatinib-insensitive. After the emerging of *KIT* secondary mutations, the ORR and PFS of exon 11-mutated patients to Imatinib was impaired (ORR: 36.7% vs. 73.2% vs. 38%; median PFS: 9 vs. 58 vs. 25 months) (**Figure 1C**, **1D**), indicating the acquisition of Imatinib resistance. Therefore, we concluded three representative categories of GIST patients according to their *KIT* status and responses to Imatinib, i.e., Imatinib primary sensitive group (exon 11 mutations), Imatinib primary insensitive group (exon 9 mutations), and Imatinib secondary resistant group (exon 11 mutations plus secondary mutations). Since acquired resistance has been a major reason that impairs the responses to Imatinib, we first investigated those individuals, in which the dominant forms of secondary *KIT* mutations for exon 13 and 17 were V654A and N822K, which was in accordance with our previous findings in a 50-case GIST patient cohort [22].

GIST-T1 and GIST-882 were two cell lines harboring primary *KIT* mutations. Since GIST-T1 carried a *KIT* exon 11-560_578del heterozygous mutation, it has a higher sensitivity to Imatinib than GIST-882 carrying an exon 13-K642E homozygous mutation. To decipher whether the secondary mutations we observed in patient cohort were involved in the acquired resistance to Imatinib, we performed lentiviruses-directed transfection of *KIT* exon 13-V654A or exon 17-N822K into GIST-T1/GIST-882 cells (**Figure 1E**). According to cell viability assay, V654A/N882K transfection significantly impaired sensitivity to Imatinib, while wild-type

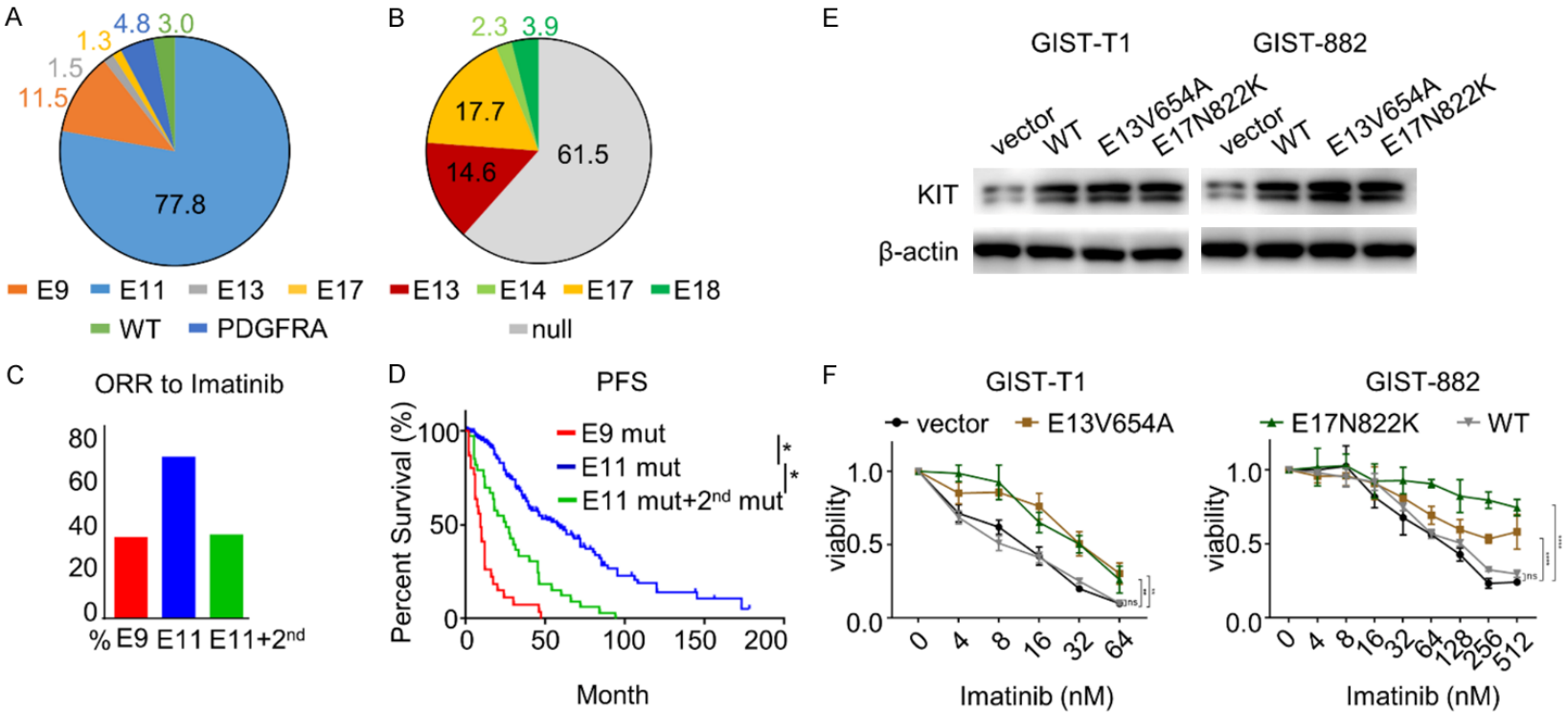

Figure 1. Specific mutations of *KIT* in GIST were associated with acquired Imatinib resistance. (A) Distribution of *KIT/PDGFRA* mutations in GIST population. (B) Distribution of secondary mutations in *KIT* exon 11 mutant-GIST patients developed resistance to Imatinib. (C) ORR (overall response rate) and (D) PFS (progression-free survival) for different *KIT* gene types. (E) Establishment of *KIT* expressing cell lines with lentivirus transfection. (F) Viability curve of GIST cells overexpressing wild type-, E13V654A-, or E17N882K-KIT after 72 hours exposure to Imatinib. All experiments were repeated three times independently. $^{*}P<0.05$.

Table 1. IC_{50} values for Imatinib in GIST cell groups

GIST cell line	IC_{50} (nM)			
	vector	E13V654A-*KIT*	E17N822K-*KIT*	WT-*KIT*
GIST-T1	16.83	28.62	30.70	16.02
GIST-882	33.49	130.19	604.8	44.89

Abbreviations: E13V654A, exon 13-V654A; E17N822K, exon 17-N822K; WT, wild-type.

(WT) *KIT* expressing groups displayed comparable sensitivity to vector groups (**Figure 1F**). The IC_{50} values for GIST cells to Imatinib were shown in **Table 1**. These data suggested that WT-*KIT* had a minimum impact on the sensitivity to Imatinib, while the acquisition of specific *KIT* mutations (i.e., exon 13-V654A and exon 17-N822K) contributed to GIST's acquired resistance to Imatinib. We also verified that Imatinib failed to increase phenotypic characteristics of the GIST-T1 and GIST-882 cells expressing E13V654A and E17N822K forms of KIT, including cell apoptosis, cycle, migration, invasion, plate clone formation, and wound-healing assay experiments which were presented in Supplementary Figures 1, 2, 3.

KIT exon 13-V654A and exon 17-N822K mutations contributed to Imatinib resistance by inducing PI3K-Akt activation in GIST cells

In order to explore the effects of *KIT* secondary mutations on the molecular characteristics of GIST, we performed RNA-sequencing for the groups stably overexpressing exon 13-V654A- or exon 17-N822K-mutated KIT, and investigated their expressional diversities. For GIST-T1, 2706 genes (1681 upregulated and 1025 downregulated) were differentially expressed between V654A and vector groups, while 1664 genes (971 upregulated and 693 downregulated) were differentially expressed between N822K and vector groups. For GIST-882, 3532 genes (1864 upregulated and 1668 downregulated) were differentially expressed between V654A and vector groups, while 1411 genes (972 upregulated and 439 downregulated) were differentially expressed between N822K and vector groups (**Figure 2A**). By referring to KEGG database, we performed pathway enrichment analysis for V654A- and N822K-transfected groups. Differentially expressed genes were mainly distributed in pathways stimulating carcinogenic progression and aggressiveness, among which PI3K-Akt signaling was consistently enriched for all four pairs of comparisons (**Figure 2B**), providing potential clues that these *KIT* secondary mutations contributed to Imatinib-resistance through stimulating PI3K-Akt signaling.

For verification, we verified the activation of PI3K-Akt signaling under different *KIT* mutational status. In accordance with total KIT level, the expressional intensity of phosphorylated KIT was higher in WT, V654A and N822K groups. While the total Akt and S6 expressions remained unaffected, p-Akt and p-S6 were evidently elevated in WT, V654A and N822K groups. More importantly, the administration of Imatinib (16 nM in GIST-T1, 64 nM in GIST-882, 72 hours) failed to quench the phosphorylation of KIT/Akt/S6 in V654A and N822K groups as succeed in vector and WT groups (**Figure 3A**). Furthermore, we tested the combination of Imatinib with the PI3K-Akt pathway inhibitor BEZ235 in V654A/N882K transfected groups. The overactivation of PI3K-Akt signaling induced by *KIT* secondary mutations was rescued by BEZ235 (**Figure 3B**), while BEZ235 augmented the growth-inhibiting efficacy of Imatinib (**Figure 3C**), emphasizing that exon 13-V654A and exon 17-N822K mutations contributed to Imatinib resistance by stimulating PI3K-Akt signaling.

Additionally, we constructed Imatinib-resistant GIST-T1R and GIST-882R sub-cells by continuously culturing the progenitor cell lines with low-dose (16 nM) to high-dose (400 nM) Imatinib for 6 months. A resistance to Imatinib was induced in both cell lines (Supplementary Figure 4A), while western blot assay showed that Imatinib with the same concentration as in progenitor cells (16 nM in GIST-T1, 64 nM in GIST-882, 72 hours) failed to suppress PI3K-Akt signaling in these resistant cells (Supplementary Figure 4B), supporting the notion that activated PI3K-Akt signaling contributed to Imatinib resistance in GIST.

Evaluation of substitutive inhibitors in GIST cells harboring Imatinib-resistant KIT mutations

With the rapid development of precision medicine, a series of new agents (such as Sunitinib, Regorafenib, Avapritinib and Ripretinib) targeting oncogenic tyrosine kinases have been developed for the treatment of KIT-related can-

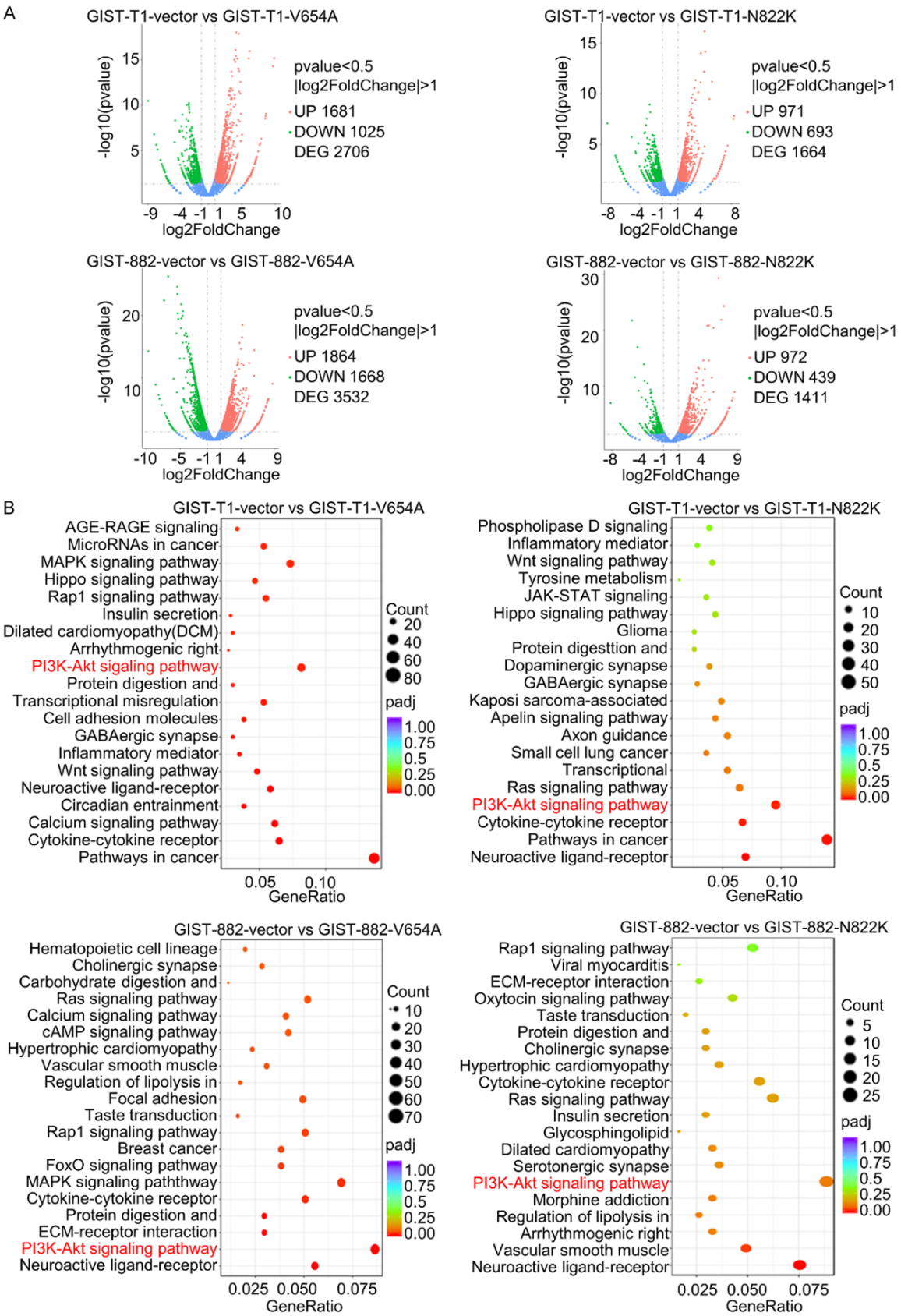

Figure 2. Dysregulated downstream pathways induced by two crucial *KIT* mutations. (A) Differentially expressed genes and (B) significantly enriched pathways comparing E13V654A/E17N822K-KIT with vector groups were demonstrated for GIST-T1/GIST-882 cells.

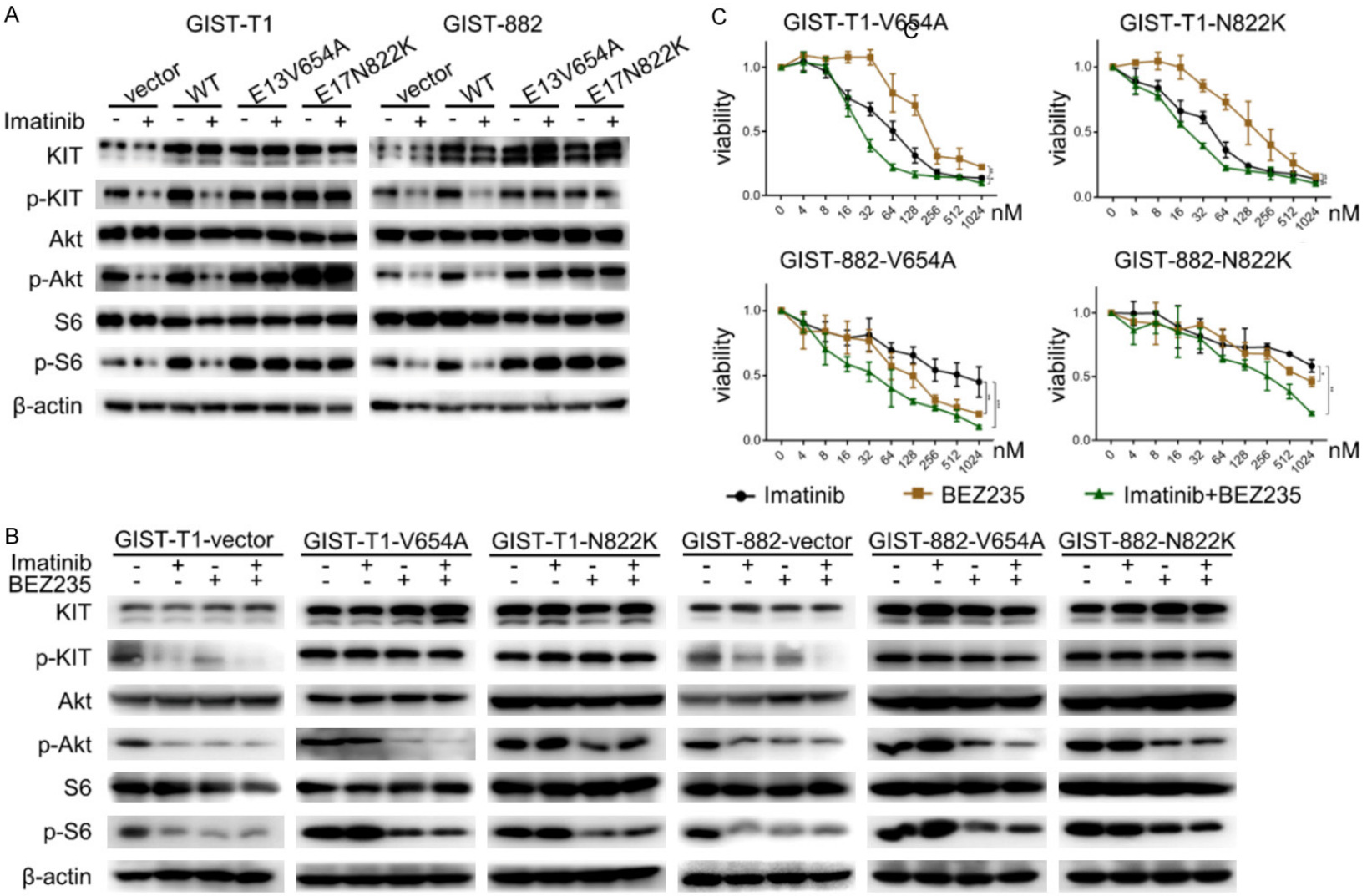

Figure 3. The activation of PI3K-Akt signaling under different *KIT* status. Western blot-quantified expression of p-KIT, p-Akt and p-S6 in (A) Imatinib-treated GIST cells transfected with E13V654A-KIT (exon 13-V654A) or E17N822K-KIT (exon 17-N822K), or (B) Imatinib and/or BEZ235-treated GIST cells transfected with E13V654A/E17N822K-KIT. (C) Viability curve of GIST cells transfected with E13V654A/E17N822K-KIT after 72 hours exposure to Imatinib with or without BEZ235.

Table 2. IC_{50} values for the four KIT-inhibiting TKIs in GIST cell groups

	IC_{50} (nM)					
	GIST-T1 -vector	GIST-T1 -V654A	GIST-T1 -N822K	GIST-882 -vector	GIST-882 -V654A	GIST-882 -N822K
Sunitinib	15.91	13.02	61.05	4.17	29.34	>1000
Regorafenib	88.97	134.50	13.29	116.20	80.27	18.07
Avapritinib	139.70	213.10	30.50	161.70	221.40	119.50
Ripretinib	53.21	>1000	19.53	470.20	1972	345.30

cers, and were currently under evaluation for potential clinical applications. Consequently, we evaluated the inhibition efficiency of the above four newly developed TKIs (tyrosine kinase inhibitors) against Imatinib-sensitive or -resistant GIST cellular groups.

In GIST-T1, when compared with vector (exon 11 mutation) group, IC_{50} values of V654A (exon 11+13 mutation) group were apparently higher for Regorafenib/Avapritinib/Ripretinib and lower for Sunitinib, while IC_{50} values of N822K (exon 11+17 mutation) group were higher for Sunitinib and lower for Regorafenib/Avapritinib/Ripretinib. In contrast, in GIST-882, when compared with vector (exon 13 mutation) group, IC_{50} values of V654A (exon 13+13 mutation) group were higher for Sunitinib/Avapritinib/Ripretinib, while IC_{50} values of N822K (exon 13+17 mutation) group were higher for Sunitinib and lower for Regorafenib/Avapritinib/Ripretinib (**Table 2**). These inconsistencies between two cell lines might be due to the diverse sensitivity endowed by their original *KIT* status (GIST-T1, *KIT* exon 11 mutation (560_578 deletion), Imatinib sensitive; GIST-882, *KIT* exon 13 mutation (K642E), Imatinib insensitive). Concomitantly, these data suggested that after acquiring *KIT* secondary mutation-associated Imatinib resistance, Sunitinib was a better option for *KIT* secondary exon 13 mutations, while Regorafenib/Avapritinib/Ripretinib had better performance for *KIT* secondary exon 17 mutations (**Figure 4A**).

On the other hand, these TKIs' pathway-inhibitive efficiency in parental and Imatinib-resistant GIST cells was also assessed by western blot. In line with the IC_{50} spectrum, secondary mutation-induced KIT phosphorylation and PI3K-Akt activation were more efficiently inhibited by Sunitinib for secondary exon 13 mutations or by Regorafenib/Avapritinib/Ripretinib for exon 17 mutations (**Figure 4B**).

Anti-tumor effects of TKIs in Imatinib-resistant GIST PDXs

Although we have previously proved the efficacy of multiple inhibitors in GIST cells harboring *KIT* secondary mutations, more powerful in vivo evidences remained to be achieved. For further validation, we established two PDX models (namely, GIST-1 and GIST-2) by applying lesions from Imatinib-resistant GIST patients. By referring to a literature concerning in vivo drug concentrations [23], we tested the anticancer efficacy of above-mentioned agents (Imatinib, Sunitinib, Regorafenib, Avapritinib and Ripretinib). For PDX-GIST-1 which carries *KIT* exon 11 (546_554 deletion) and *KIT* exon 17 (Y823D) mutations (primary Imatinib sensitive + acquired resistance), the efficacy of Imatinib was compromised, while Avapritinib and Regorafenib showed significantly higher tumor growth inhibition than other agents (**Figure 5A**). For PDX-GIST-2 that carries *KIT* exon 9 502-503 duplication mutation (primary Imatinib insensitive), a resistance to Imatinib was also observed. The best inhibitory effects were achieved by Avapritinib/Sunitinib and followed by Regorafenib, while Ripretinib had only weak antitumor effects (**Figure 5B**). All these regimens displayed comparable adverse effect on body weight as Imatinib, indicating acceptable toxicity (Supplementary Figure 5A). In addition to the reduction in tumor size, microscopic evaluation showed that Avapritinib/Regorafenib/Sunitinib treatment for PDX-GIST-1, as well as Sunitinib/Avapritinib/Regorafenib treatment for PDX-GIST-2, exhibited reductions in nuclear density (Supplementary Figure 5B). This reduction was due to mucus-like degeneration and found in GIST and other mesenchymal tumors, and the main feature was that connective tissue mucosa replaced tumor cells [23].

We then compared the molecular changes induced by treatment of these TKIs. KIT phosphorylation and PI3K-Akt activation (represented by p-Akt and p-S6) were strongly repressed by Sunitinib/Regorafenib/Avapritinib yet mildly or seldom affected by other agents including Imatinib (**Figure 5C**, **5D**). These data were in agreement with in vitro studies, validating that these TKIs exerted similar inhibitive effect on PI3K-Akt signaling as BEZ235, and blocked tumor growth induced by *KIT* mutation and subsequent PI3K-Akt in Imatinib-tolerant GIST. The

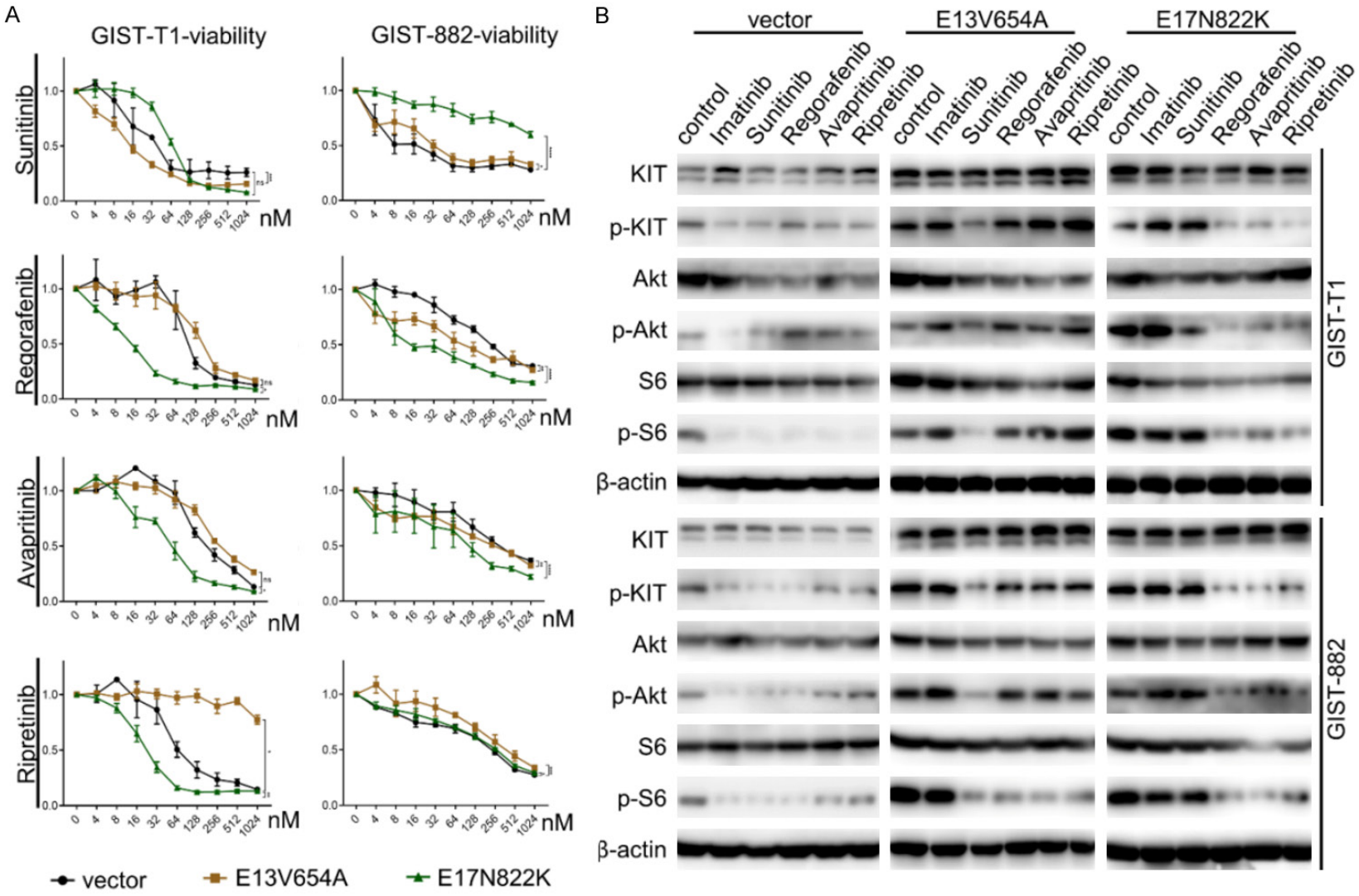

Figure 4. Inhibition efficiency of Sunitinib, Regorafenib, Avapritinib and Ripretinib against Imatinib-sensitive or -resistant GIST cell groups. A. Viability curve of GIST-T1/GIST-882 cells after 72 hours exposure to Sunitinib, Regorafenib, Avapritinib and Ripretinib. B. Western blot quantification of protein expressional intensity of p-KIT, p-Akt and p-S6 in vector, E13V654A and E17N822K for GIST-T1/GIST-882 cells after exposure to Imatinib, Sunitinib, Regorafenib, Avapritinib and Ripretinib. All experiments were repeated three times independently.

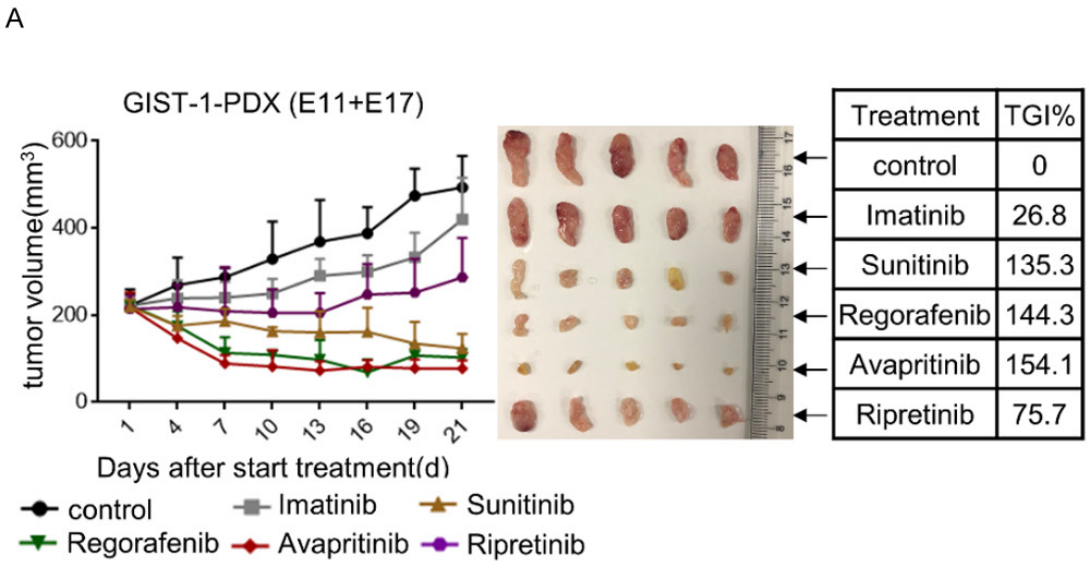

Treatment	TGI%
control	0
Imatinib	26.8
Sunitinib	135.3
Regorafenib	144.3
Avapritinib	154.1
Ripretinib	75.7

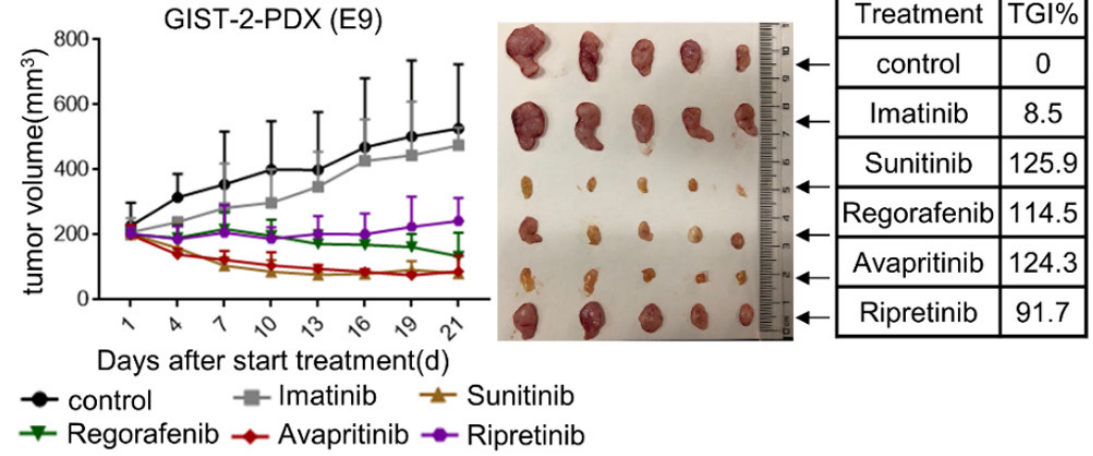

Treatment	TGI%
control	0
Imatinib	8.5
Sunitinib	125.9
Regorafenib	114.5
Avapritinib	124.3
Ripretinib	91.7

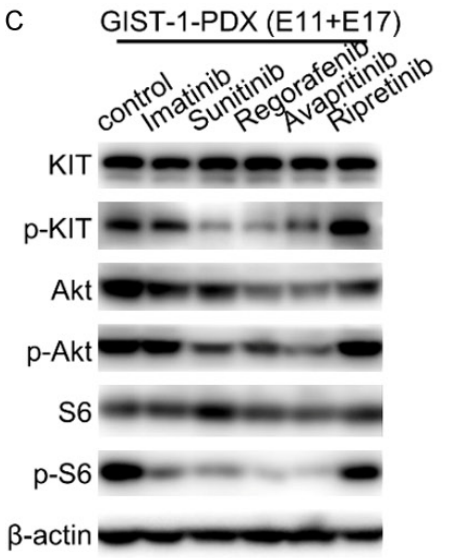

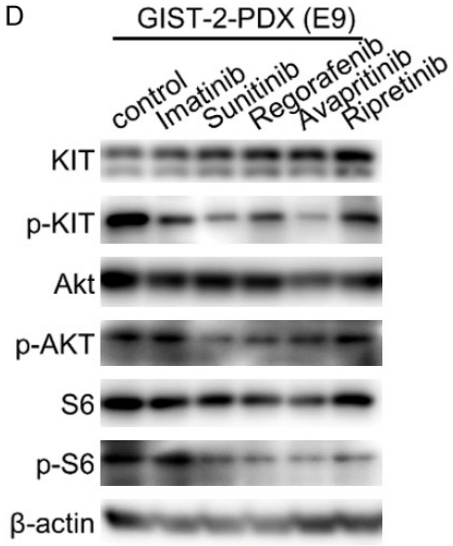

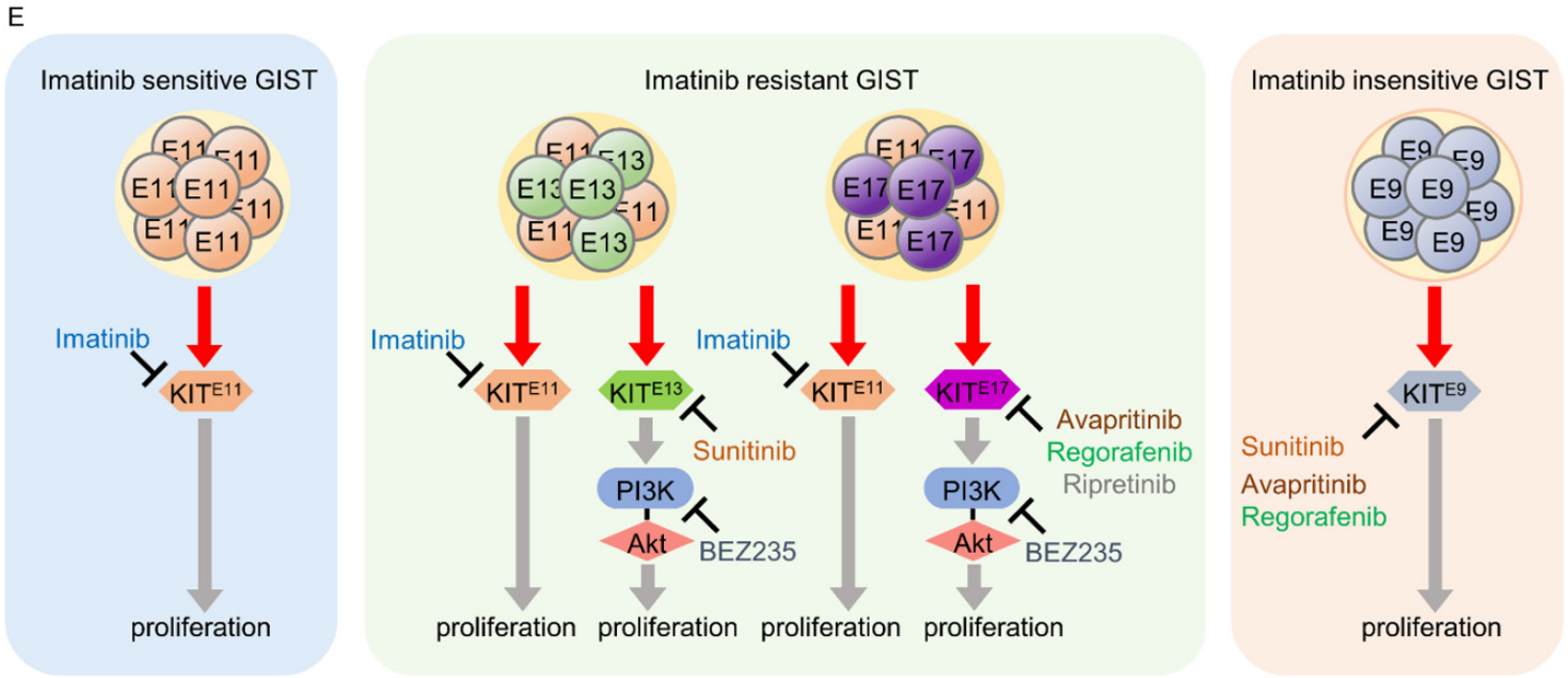

Figure 5. Anti-tumor effects of TKIs in Imatinib-resistant GIST PDX. Antitumor activity of TKIs in human GIST PDX models with (A) *KIT* exon 11 (del546-554) plus exon 17 (Y823D) or (B) *KIT* exon 9 (dup502-503) mutations. Lysates were extracted from GIST-1 (C) and GIST-2 (D) xenografts after 21 days of treatment with the corresponding inhibitors and analyzed by western blotting to explore the downstream signaling responses. (E) A schematic diagram of the molecular mechanisms of acquired resistance revealed in this study.

resistance mechanism and spectrum for proper regimens were systematically summarized in **Figure 5E**.

Taken together, we concluded that Sunitinib/Regorafenib/Avapritinib were powerful regimens against Imatinib-tolerant GIST. The high tumor growth inhibition for both cell lines and PDXs indicated that under tolerable dosages, a complete therapeutic coverage by selecting these regimens was achievable for Imatinib-tolerant populations, including both *KIT* primary and secondary mutation-related resistance.

Discussion

The average annual incidence of gastrointestinal stromal tumor (GIST) was about 19 per million people [24]. As a pioneer of targeted therapy for solid tumors, Imatinib has been used in patients with recurrent metastatic GIST, with an overall response rate of up to 50% [25]. However, although most targeted drugs respond initially, the inevitable emergence of resistance has been a major problem that prominently hinders therapeutic responses. After receiving Imatinib treatment, approximately 9-13% of GIST patients developed primary resistance [26], which is currently considered to be closely related to the genotype of wild-type, *KIT* gene exon 9 mutations, and *PDGFRA* gene exon 18 D842V mutation [15, 27]. Furthermore, most patients responded sensitively to Imatinib developed the acquired resistance during treatment, which severely impaired the rate of complete remission in advanced GIST populations. Secondary gene mutations, predominantly happened on *KIT* exon 13/17, were detected in 46.7-83% of GIST patients that acquired resistance [15-17, 27-29], suggesting that secondary mutations are an important cause of acquired resistance. In this study, we applied multiple models to evaluate the impact of *KIT* secondary mutations on acquired Imatinib resistance and their potential therapeutic regimens. V654A and N822K were the most common type of *KIT* exon 13 and exon 17 mutations, whose transfections in GIST cells mimicked the acquisition of Imatinib resistance. Our data confirmed that the sensitivity of Imatinib in GIST cells was decreased after acquiring these secondary mutations, which was in accordance with previous research [30].

We validated that the acquired resistance to Imatinib induced by specific *KIT* mutations was most likely to be originated from an overactivation of PI3K-Akt signaling, as indicated by previous studies [31]. Notably, the overactivation of PI3K-Akt signaling was also observed in GIST cell lines with induced Imatinib resistance. Although we did not assess the genomic changes of *KIT* in these cells, the administration of the PI3K-Akt pathway inhibitor BEZ235, in certain degrees, augmented the anti-GIST efficacy of Imatinib against V654A and N822K for both cell lines, validating that PI3K-Akt signaling contributed to this resistance, and the combination with PI3K-Akt inhibitors might be an option in rescuing secondary mutation-associated Imatinib resistance.

However, the development of PI3K-Akt inhibitors in clinical practice was lagged behind due to failures in multiple trials [32], while it has also been reported that KIT protein was still the main dependence for Imatinib-resistant GIST cell lines to activate downstream signals and maintain growth [15]. As inspired by this KIT-dependency, seeking other tyrosine kinase inhibitors targeting a broader spectrum of *KIT* secondary mutations could be considered as a better strategy than PI3K-Akt inhibitors in order to overcome Imatinib resistance at current stage [30]. Increasing evidences suggested that several TKIs, including Sunitinib and Regorafenib, displayed promising prospects in multiple types of cancer [15]. These efforts led to the approval of Sunitinib and Regorafenib as second-line and third-line therapies respectively, for patients with advanced GIST [33-36]. GIST patients with Imatinib-resistant tumors are treated with Sunitinib, which potently inhibits *KIT* ATP-binding pocket mutations [37]. However, Sunitinib is ineffective against A-loop mutants, which account for 50% of Imatinib-resistant mutations [38]. This may explain why overall response rates (ORR) are low (7%) and median progression-free survival (PFS) is short (6.2 months) [39]. Regorafenib was approved as third-line therapy, but showed only moderate activity, with ORR of 4.5% and median PFS of 4.8 months [38].

A series of other multi-kinase inhibitors are currently assessed by phase I to phase III clinical studies [40, 41], among which two TKIs are found with promising perspectives. The first is

Avapritinib (BLU-285, Blueprint Medicines), an oral, highly-selective and potent investigational inhibitor of *KIT* and *PDGFRA* activation loop mutation [42]. In vitro, Avapritinib disrupts KIT signaling as assessed by inhibition of both KIT phosphorylation and activation of downstream proteins such as Akt in human mast cell and leukemia cell lines. In vivo, Avapritinib achieves dose-dependent tumor growth inhibition in a mouse model of systemic mastocytosis (SM). Moreover, Avapritinib also inhibits *PDGFRA* D842V [38], the mutation responsible for one out of five primary gastric GIST, for which there is no effective treatment available [26]. The other one is Ripretinib, a switch control type II inhibitor of KIT, which arrests KIT in an inactive state regardless of its activating mutations, such as *KIT* D816V [43]. Several additional oncogenic kinases, including FLT-3, PDGFRA, PDGFRB, KDR, TIE2 and FMS, are also recognized by Ripretinib [44-46].

Thus, Avapritinib and Ripretinib were currently under clinical investigation (NCT02508532, NCT03465722, NCT03862885 for Avapritinib, NCT04148092, NCT03353753, NCT036735-01, NCT02571036 for Ripretinib) in solid tumor patients (including GIST). Although Sunitinib, Regorafenib, Avapritinib and Ripretinib have been recognized as promising agents against GIST, their antitumor mechanisms and feasible types of *KIT* status still remained unexplored. Thus, we explored their therapeutic potential against Imatinib-resistant GIST, and proposed they were suitable options for *KIT* exon 13 and exon 17 secondary mutations. Notably, an inconsistency between GIST-T1- and GIST-882-related groups was observed regarding the responses to Imatinib and/or BEZ235, as well as to the other four KIT-targeted inhibitors. Since GIST-T1 carried a *KIT* exon 11-560_578 deletion while GIST-882 carried an exon 13-K642E mutation, it is of note that GIST-T1 resembled the primarily sensitive type while GIST-882 resembled the primarily insensitive type of GIST, which explained their diversity to drug treatments [18, 19].

For *KIT* exon 13-mutation related Imatinib resistance, a previous report pointed out that Ripretinib was most effective to GIST-430 cells carrying *KIT* exon 11 and 13-V654A mutations [43], yet our research exhibited that Ripretinib was less effective to *KIT* exon 13 mutations. For *KIT* exon 17 mutation related Imatinib-resistance, although Ripretinib showed strong antitumor effects in vitro in Imatinib-resistant GIST cells with *KIT* exon 17-N822K mutation, its inhibition (represented by tumor growth inhibition) on the in vivo growth of PDX-GIST-1 carrying *KIT* exon 11 and exon 17-Y823D mutations was less efficient than Avapritinib, Regorafenib or even Sunitinib. Therefore, higher dosages of Ripretinib may be required to achieve the same effect against Imatinib-resistant GIST as Regorafenib and Avapritinb, which complied with a report that 50 mg/Bid was needed in the body to achieve an eminent antitumor effect [43]. Despite these diversities, investigation for both cells consistently indicated that Sunitinib was an option for *KIT* secondary exon 13 mutations, while Regorafenib/Avapritinib/Ripretinib were better candidates for secondary exon 17 mutations (with acquired Imatinib resistance). Moreover, our findings suggested that Sunitinib was also effective for PDX-GIST-1 carrying *KIT* exon 17 mutations, which finding was in consistent with a previous research [47]. However, due to the diversity between cellular and PDX data, it remained to be answered whether Suntinib could be considered applicable for both *KIT* exon 13 and exon 17 mutations.

Apart from exon 13 and exon 17 mutations, we also verified the anti-tumor effects of the four TKIs for GIST (PDX-GIST-2) that carried *KIT* exon 9 mutations. As previously described, GIST *KIT* exon 9 mutation was considered to be a primary insensitive phenotype. Both primary insensitivity (represented by *KIT* exon 9) and acquired resistance (represented by *KIT* exon 11+exon 13, or exon 11+exon 17 mutations) to Imatinib could be effectively overcame by combining these TKIs, suggesting that although with heterogenic efficacies, these TKIs were valuable therapeutic complements or even potential substitutions for Imatinib. Thus, it is worthy to keep promoting the development of relevant clinical trials.

In conclusion, we proved that the overactivation of PI3K-Akt signaling induced by multiple *KIT* mutations mediated Imatinib-resistance in GIST. The inhibition of PI3K-Akt signaling restored the efficacy of Imatinib, while other newly developed TKIs, especially Sunitinib, Regorafenib and Avapritinib, were realistic choice for clinical applications. By shedding light upon the new strategies for major problem of current targeted therapy, our work expanded

the armory against Imatinib-resistant GIST, which might benefit a large number of patients.

Conclusion

Through applying multiple GIST models, we unveiled the involvement of specific *KIT* mutations in activating PI3K-Akt signaling and inducing Imatinib resistance. By evaluating the preclinical efficacy of PI3K-Akt inhibitor BEZ235 as well as several newly developed TKIs, we verified that these agents were potential options to overcome Imatinib resistance for GIST patients in the future.

Acknowledgements

We deeply appreciate Drs. Yuexiang Wang (Changzheng Hospital, Shanghai, China), Congcong Ji, Ying Wu and Yanyan Li (Peking University Cancer Hospital & Institute) for kind suggestions and generous help in providing experimental materials during this study. This work was supported by the National Natural Science Foundation of China (No. 81802327, No. 81902514), the third round of public welfare development and reform pilot projects of Beijing Municipal Medical Research Institutes (Beijing Medical Research Institute, 2019-1), and the National Key Research and Development Program of China (2018YFC1313304).

Disclosure of conflict of interest

None.

Abbreviations

GIST, gastrointestinal stromal tumor; TKI, tyrosine kinase inhibitor; PDGFRA, platelet-derived growth factor receptor alpha; PDX, patient-derived xenograft; ORR, overall response rate; PFS, progression-free survival; WT, wild-type; KEGG, Kyoto Encyclopedia of Genes and Genomes; PD, progressive disease; PR, partial response; CR, complete response; SD, stable disease.

Address correspondence to: Jian Li and Cheng Zhang, Department of Gastrointestinal Oncology, Key Laboratory of Carcinogenesis and Translational Research (Ministry of Education/Beijing), Peking University Cancer Hospital & Institute, Fu-Cheng Road 52, Haidian District, Beijing 100142, China. Tel: +86-10-88196561; E-mail: oncogene@163.com (JL); qenya_z@bjmu.edu.cn (CZ); Jing Gao, National Cancer Center/National Clinical Research Center for Cancer/Cancer Hospital & Shenzhen Hospital, Chinese Academy of Medical Sciences and Peking Union Medical College, Bao-He Road 113, Longgang District, Shenzhen 518000, Guangdong, China. E-mail: gaojing_pumc@163.com

References

[1] Miettinen M and Lasota J. Gastrointestinal stromal tumors: pathology and prognosis at different sites. Semin Diagn Pathol 2006; 23: 70-83.

[2] Hirota S, Isozaki K, Moriyama Y, Hashimoto K, Nishida T, Ishiguro S, Kawano K, Hanada M, Kurata A, Takeda M, Muhammad Tunio G, Matsuzawa Y, Kanakura Y, Shinomura Y and Kitamura Y. Gain-of-function mutations of c-kit in human gastrointestinal stromal tumors. Science 1998; 279: 577-580.

[3] Mucciarini C, Rossi G, Bertolini F, Valli R, Cirilli C, Rashid I, Marcheselli L, Luppi G and Federico M. Incidence and clinicopathologic features of gastrointestinal stromal tumors. A population-based study. BMC cancer 2007; 7: 230.

[4] Bauer S, Hartmann J, de Wit M, Lang H, Grabellus F, Antoch G, Niebel W, Erhard J, Ebeling P, Zeth M, Taeger G, Seeber S, Flasshove M and Schütte J. Resection of residual disease in patients with metastatic gastrointestinal stromal tumors responding to treatment with imatinib. Int J Cancer 2005; 117: 316-325.

[5] Ng EH, Pollock RE, Munsell MF, Atkinson EN and Romsdahl MM. Prognostic factors influencing survival in gastrointestinal leiomyosarcomas. Implications for surgical management and staging. Ann Surg 1992; 215: 68-77.

[6] DeMatteo RP, Lewis JJ, Leung D, Mudan SS, Woodruff JM and Brennan MF. Two hundred gastrointestinal stromal tumors: recurrence patterns and prognostic factors for survival. Ann Surg 2000; 231: 51-58.

[7] Joensuu H, Hohenberger P and Corless CL. Gastrointestinal stromal tumour. Lancet 2013; 382: 973-983.

[8] Joensuu H, Eriksson M, Sundby Hall K, Reichardt A, Hartmann JT, Pink D, Ramadori G, Hohenberger P, Al-Batran SE, Schlemmer M, Bauer S, Wardelmann E, Nilsson B, Sihto H, Bono P, Kallio R, Junnila J, Alvegard T and Reichardt P. Adjuvant Imatinib for high-risk GI stromal tumor: analysis of a randomized trial. J Clin Oncol 2016; 34: 244-250.

[9] Judson I and Demetri G. Advances in the treatment of gastrointestinal stromal tumours. Ann Oncol 2007; 18 Suppl 10: x20-24.

[10] Din OS and Woll PJ. Treatment of gastrointestinal stromal tumor: focus on Imatinib mesylate. Ther Clin Risk Manag 2008; 4: 149-162.

[11] Dirnhofer S and Leyvraz S. Current standards and progress in understanding and treatment of GIST. Swiss Med Wkly 2009; 139: 90-102.

[12] Demetri GD, von Mehren M, Blanke CD, Van den Abbeele AD, Eisenberg B, Roberts PJ, Heinrich MC, Tuveson DA, Singer S, Janicek M, Fletcher JA, Silverman SG, Silberman SL, Capdeville R, Kiese B, Peng B, Dimitrijevic S, Druker BJ, Corless C, Fletcher CD and Joensuu H. Efficacy and safety of Imatinib mesylate in advanced gastrointestinal stromal tumors. N Engl J Med 2002; 347: 472-480.

[13] Blanke CD, Demetri GD, von Mehren M, Heinrich MC, Eisenberg B, Fletcher JA, Corless CL, Fletcher CD, Roberts PJ, Heinz D, Wehre E, Nikolova Z and Joensuu H. Long-term results from a randomized phase II trial of standard-versus higher-dose Imatinib mesylate for patients with unresectable or metastatic gastrointestinal stromal tumors expressing KIT. J Clin Oncol 2008; 26: 620-625.

[14] Desai J, Shankar S, Heinrich MC, Fletcher JA, Fletcher CD, Manola J, Morgan JA, Corless CL, George S, Tuncali K, Silverman SG, Van den Abbeele AD, van Sonnenberg E and Demetri GD. Clonal evolution of resistance to Imatinib in patients with metastatic gastrointestinal stromal tumors. Clin Cancer Res 2007; 13: 5398-5405.

[15] Heinrich MC, Corless CL, Blanke CD, Demetri GD, Joensuu H, Roberts PJ, Eisenberg BL, von Mehren M, Fletcher CD, Sandau K, McDougall K, Ou WB, Chen CJ and Fletcher JA. Molecular correlates of Imatinib resistance in gastrointestinal stromal tumors. J Clin Oncol 2006; 24: 4764-4774.

[16] Liegl B, Kepten I, Le C, Zhu M, Demetri GD, Heinrich MC, Fletcher CD, Corless CL and Fletcher JA. Heterogeneity of kinase inhibitor resistance mechanisms in GIST. J Pathol 2008; 216: 64-74.

[17] Wardelmann E, Merkelbach-Bruse S, Pauls K, Thomas N, Schildhaus HU, Heinicke T, Speidel N, Pietsch T, Buettner R, Pink D, Reichardt P and Hohenberger P. Polyclonal evolution of multiple secondary KIT mutations in gastrointestinal stromal tumors under treatment with Imatinib mesylate. Clin Cancer Res 2006; 12: 1743-1749.

[18] Tuveson DA, Willis NA, Jacks T, Griffin JD, Singer S, Fletcher CD, Fletcher JA and Demetri GD. STI571 inactivation of the gastrointestinal stromal tumor c-KIT oncoprotein: biological and clinical implications. Oncogene 2001; 20: 5054-5058.

[19] Taguchi T, Sonobe H, Toyonaga S, Yamasaki I, Shuin T, Takano A, Araki K, Akimaru K and Yuri K. Conventional and molecular cytogenetic characterization of a new human cell line, GIST-T1, established from gastrointestinal stromal tumor. Lab Invest 2002; 82: 663-665.

[20] Zhang C, Lin X, Zhao Q, Wang Y, Jiang F, Ji C, Li Y, Gao J, Li J and Shen L. YARS as an oncogenic protein that promotes gastric cancer progression through activating PI3K-Akt signaling. J Cancer Res Clin Oncol 2020; 146: 329-342.

[21] Liu Z, Chen Z, Wang J, Zhang M, Li Z, Wang S, Dong B, Zhang C, Gao J and Shen L. Mouse avatar models of esophageal squamous cell carcinoma proved the potential for EGFR-TKI afatinib and uncovered Src family kinases involved in acquired resistance. J Hematol Oncol 2018; 11: 109.

[22] Gao J, Tian Y, Li J, Sun N, Yuan J and Shen L. Secondary mutations of c-KIT contribute to acquired resistance to Imatinib and decrease efficacy of sunitinib in Chinese patients with gastrointestinal stromal tumors. Med Oncol 2013; 30: 522.

[23] Evans EK, Gardino AK, Kim JL, Hodous BL, Shutes A, Davis A, Zhu XJ, Schmidt-Kittler O, Wilson D, Wilson K, DiPietro L, Zhang Y, Brooijmans N, LaBranche TP, Wozniak A, Gebreyohannes YK, Schoffski P, Heinrich MC, DeAngelo DJ, Miller S, Wolf B, Kohl N, Guzi T, Lydon N, Boral A and Lengauer C. A precision therapy against cancers driven by KIT/PDGFRA mutations. Sci Transl Med 2017; 9: 1690.

[24] Corless CL, Barnett CM and Heinrich MC. Gastrointestinal stromal tumours: origin and molecular oncology. Nat Rev Cancer 2011; 11: 865-878.

[25] van Oosterom AT, Judson I, Verweij J, Stroobants S, Donato di Paola E, Dimitrijevic S, Martens M, Webb A, Sciot R, Van Glabbeke M, Silberman S and Nielsen OS; European Organisation for Research and Treatment of Cancer Soft Tissue and Bone Sarcoma Group. Safety and efficacy of Imatinib (STI571) in metastatic gastrointestinal stromal tumours: a phase I study. Lancet 2001; 358: 1421-1423.

[26] Zalcberg JR, Verweij J, Casali PG, Le Cesne A, Reichardt P, Blay JY, Schlemmer M, Van Glabbeke M, Brown M and Judson IR; EORTC Soft Tissue and Bone Sarcoma Group, the Italian Sarcoma Group; Australasian Gastrointestinal Trials Group. Outcome of patients with advanced gastro-intestinal stromal tumours crossing over to a daily Imatinib dose of 800 mg after progression on 400 mg. Eur J Cancer 2005; 41: 1751-1757.

[27] Debiec-Rychter M, Cools J, Dumez H, Sciot R, Stul M, Mentens N, Vranckx H, Wasag B, Prenen H, Roesel J, Hagemeijer A, Van Oosterom A and Marynen P. Mechanisms of resistance to Imatinib mesylate in gastrointestinal stromal tumors and activity of the PKC412 inhibitor against imatinib-resistant mutants. Gastroenterology 2005; 128: 270-279.

[28] Agaram NP, Besmer P, Wong GC, Guo T, Socci ND, Maki RG, DeSantis D, Brennan MF, Singer S, DeMatteo RP and Antonescu CR. Pathologic and molecular heterogeneity in imatinib-stable or imatinib-responsive gastrointestinal stromal tumors. Clin Cancer Res 2007; 13: 170-181.

[29] Antonescu CR, Besmer P, Guo T, Arkun K, Hom G, Koryotowski B, Leversha MA, Jeffrey PD, Desantis D, Singer S, Brennan MF, Maki RG and DeMatteo RP. Acquired resistance to Imatinib in gastrointestinal stromal tumor occurs through secondary gene mutation. Clin Cancer Res 2005; 11: 4182-4190.

[30] Serrano C, Marino-Enriquez A, Tao DL, Ketzer J, Eilers G, Zhu M, Yu C, Mannan AM, Rubin BP, Demetri GD, Raut CP, Presnell A, McKinley A, Heinrich MC, Czaplinski JT, Sicinska E, Bauer S, George S and Fletcher JA. Complementary activity of tyrosine kinase inhibitors against secondary kit mutations in imatinib-resistant gastrointestinal stromal tumours. Br J Cancer 2019; 120: 612-620.

[31] Wang CM, Huang K, Zhou Y, Du CY, Ye YW, Fu H, Zhou XY and Shi YQ. Molecular mechanisms of secondary Imatinib resistance in patients with gastrointestinal stromal tumors. J Cancer Res Clin Oncol 2010; 136: 1065-1071.

[32] Patel S. Exploring novel therapeutic targets in GIST: focus on the PI3K/Akt/mTOR pathway. Curr Oncol Rep 2013; 15: 386-395.

[33] Demetri GD, Heinrich MC, Fletcher JA, Fletcher CD, Van den Abbeele AD, Corless CL, Antonescu CR, George S, Morgan JA, Chen MH, Bello CL, Huang X, Cohen DP, Baum CM and Maki RG. Molecular target modulation, imaging, and clinical evaluation of gastrointestinal stromal tumor patients treated with sunitinib malate after Imatinib failure. Clin Cancer Res 2009; 15: 5902-5909.

[34] Demetri GD, Reichardt P, Kang YK, Blay JY, Rutkowski P, Gelderblom H, Hohenberger P, Leahy M, von Mehren M, Joensuu H, Badalamenti G, Blackstein M, Le Cesne A, Schoffski P, Maki RG, Bauer S, Nguyen BB, Xu J, Nishida T, Chung J, Kappeler C, Kuss I, Laurent D and Casali PG; GRID study investigators. Efficacy and safety of regorafenib for advanced gastrointestinal stromal tumours after failure of Imatinib and sunitinib (GRID): an international, multicentre, randomised, placebo-controlled, phase 3 trial. Lancet 2013; 381: 295-302.

[35] Demetri GD, van Oosterom AT, Garrett CR, Blackstein ME, Shah MH, Verweij J, McArthur G, Judson IR, Heinrich MC, Morgan JA, Desai J, Fletcher CD, George S, Bello CL, Huang X, Baum CM and Casali PG. Efficacy and safety of sunitinib in patients with advanced gastrointestinal stromal tumour after failure of imatinib: a randomised controlled trial. Lancet 2006; 368: 1329-1338.

[36] Wilhelm SM, Dumas J, Adnane L, Lynch M, Carter CA, Schutz G, Thierauch KH and Zopf D. Regorafenib (BAY 73-4506): a new oral multikinase inhibitor of angiogenic, stromal and oncogenic receptor tyrosine kinases with potent preclinical antitumor activity. Int J Cancer 2011; 129: 245-255.

[37] Yuzawa S, Opatowsky Y, Zhang Z, Mandiyan V, Lax I and Schlessinger J. Structural basis for activation of the receptor tyrosine kinase KIT by stem cell factor. Cell 2007; 130: 323-334.

[38] Yamamoto H, Tobo T, Nakamori M, Imamura M, Kojima A, Oda Y, Nakamura N, Takahira T, Yao T and Tsuneyoshi M. Neurofibromatosis type 1-related gastrointestinal stromal tumors: a special reference to loss of heterozygosity at 14q and 22q. J Cancer Res Clin Oncol 2009; 135: 791-798.

[39] Wasag B, Debiec-Rychter M, Pauwels P, Stul M, Vranckx H, Oosterom AV, Hagemeijer A and Sciot R. Differential expression of KIT/PDGFRA mutant isoforms in epithelioid and mixed variants of gastrointestinal stromal tumors depends predominantly on the tumor site. Mod Pathol 2004; 17: 889-894.

[40] Wang Y and Fletcher JA. Cell cycle and dystrophin dysregulation in GIST. Cell Cycle 2015; 14: 2713-2714.

[41] Serrano C and George S. Recent advances in the treatment of gastrointestinal stromal tumors. Ther Adv Med Oncol 2014; 6: 115-127.

[42] Gebreyohannes YK, Wozniak A, Zhai ME, Wellens J, Cornillie J, Vanleeuw U, Evans E, Gardino AK, Lengauer C, Debiec-Rychter M, Sciot R and Schoffski P. Robust activity of avapritinib, potent and highly selective inhibitor of mutated KIT, in patient-derived xenograft models of gastrointestinal stromal tumors. Clin Cancer Res 2019; 25: 609-618.

[43] Smith BD, Kaufman MD, Lu WP, Gupta A, Leary CB, Wise SC, Rutkoski TJ, Ahn YM, Al-Ani G, Bulfer SL, Caldwell TM, Chun L, Ensinger CL, Hood MM, McKinley A, Patt WC, Ruiz-Soto R, Su Y, Telikepalli H, Town A, Turner BA, Vogeti L, Vogeti S, Yates K, Janku F, Abdul Razak AR, Rosen O, Heinrich MC and Flynn DL. Ripretinib (DCC-2618) is a switch control kinase inhibitor of a broad spectrum of oncogenic and drug-resistant KIT and PDGFRA variants. Cancer Cell 2019; 35: 738-751, e739.

[44] Villanueva MT. Ripretinib turns off the switch in GIST. Nat Rev Cancer 2019; 19: 370.

[45] Mazzocca A, Napolitano A, Silletta M, Spalato Ceruso M, Santini D, Tonini G and Vincenzi B. New frontiers in the medical management of gastrointestinal stromal tumours. Ther Adv Med Oncol 2019; 11: 1758835919841946.

[46] Falkenhorst J, Hamacher R and Bauer S. New therapeutic agents in gastrointestinal stromal tumours. Curr Opin Oncol 2019; 31: 322-328.

[47] Na YS, Ryu MH, Yoo C, Lee JK, Park JM, Lee CW, Lee SY, Shin YK, Ku JL, Ahn SM and Kang YK. Establishment and characterization of patient-derived xenograft models of gastrointestinal stromal tumor resistant to standard tyrosine kinase inhibitors. Oncotarget 2017; 8: 76712-76721.

Supplementary Methods

Plate clone formation experiment

GIST-T1 and GIST-882 cells were inoculated in 6-well plates with 2 mL of IMDM medium (20% FBS). In total, 1,000 cells were plated in each well. Cells were kept in the incubator at 37°C, 5% CO_2 for 14 days (GIST-T1) or 28 days (GIST-882). The medium in each well was changed every 3 days. On the 14th (or 28th) day, 4% paraformaldehyde was used for the fixation of cells. Then crystal violet was utilized for the staining of cells. The colony numbers of cells in each well were counted under an optical microscope (Nikon, Japan). A colony with more than 50 cells was considered as one colony formation. The experiment was repeated three times.

Transwell experiment

A total of 2×10^3 GIST-T1 or GIST-882 cells were suspended in 100 μL of serum-free IMDM medium. Cells were then added into the upper chamber of the Transwell (Corningcostar 3422 and BD 353096, USA) in a 24-well plate containing 500 μL of IMDM medium (20% FBS). Cells were maintained at 37°C, 5% CO_2 for 48 to 72 hours. After incubation, cells were then fixed with 4% paraformaldehyde, and the cells in the upper chamber were wiped off by cotton swab. Cells of the lower chamber were stained by crystal violet. The number of migrating and invading cells was measured under a microscope in three random fields. The experiment was repeated three times.

Wound-healing assay

About 5×10^5 GIST-T1 or GIST-882 cells per well were added to the 6-well plate and incubated overnight in a 37°C incubator until the cells were confluent. A 200 μL pipette tip was used to make a scratch in the middle of the cells of the 6-well plate. After that, the cells were washed with PBS (HyClone SH30256.01B, USA) and then recorded wound area under a microscope (5×). After culturing in serum-free medium for 24 to 48 hours, the wound area of cells was recorded. The experiment was repeated three times.

Apoptosis and cell cycle analysis

GIST-T1 or GIST-882 cells were harvested and washed with PBS. The cells were suspended with 75% ethanol and fixed overnight at 4°C. Next day, the cells were collected and stained with propidium iodide (Solarbio C8470, China) to analyze cell cycle process using flow cytometry (BD AccuriTM C6, USA). Additionally, the cells were suspended with binding buffer (Dojindo AD11, Japan), stained with annexin 633 and PI, and then cell apoptosis rate was analyzed by the flow cytometry. The experiment was repeated three times.

Supplementary Table 1. The clinicopathological characteristics of 2273 Chinese GIST patients

Characteristics	No. of patient (%)	*KIT* primary mutation				*KIT* secondary mutation				*PDGFRA* mutation		Wild-type
		exon 11	exon 9	exon 13	exon 17	exon 11+13	exon 11+14	exon 11+17	exon 11+18	exon 12	exon 18	
	2273	1719 (75.6)	263 (11.5)	33 (1.5)	30 (1.3)	19 (0.8)	3 (0.1)	23 (1.0)	5 (0.2)	15 (0.7)	94 (4.1)	69 (3.0)
gender												
male	1333 (58.6)	990 (57.6)	159 (60.5)	22 (66.7)	22 (73.3)	13 (68.4)	2 (66.7)	12 (52.2)	4 (80.0)	9 (60.0)	60 (63.8)	40 (58.0)
female	940 (41.4)	729 (42.4)	104 (39.5)	11 (33.3)	8 (26.7)	6 (31.6)	1 (33.3)	11 (47.8)	1 (20.0)	6 (40.0)	34 (36.2)	29 (42.0)
age												
median (years)	56	58	55	62	60	56	61	54	58	55.5	55	51.5
range (years)	7-90	13-90	24-84	31-76	26-82	32-83	57-67	36-74	55-66	31-72	21-80	7-88
site												
gastric	847 (37.3)	709 (42.2)	18 (6.8)	6 (18.2)	4 (13.3)	8 (42.1)	1 (33.3)	3 (13.0)	5 (100)	10 (66.7)	64 (68.1)	19 (27.5)
small bowel	710 (31.2)	482 (28.0)	172 (65.4)	16 (48.5)	14 (46.7)	6 (31.6)	0	12 (52.2)	0	0	3 (3.2)	5 (7.3)
others	329 (14.5)	241 (14.0)	38 (14.5)	11 (33.3)	6 (20.0)	3 (15.8)	2 (66.7)	6 (26.1)	0	3 (20.0)	8 (8.5)	11 (15.9)
missing data	387 (17.0)	287 (16.7)	35 (13.3)	0	6 (20.0)	2 (10.5)	0	2 (8.7)	0	2 (13.3)	19 (20.2)	34 (49.3)
diameter												
<5 cm	236 (10.4)	191 (11.1)	18 (6.8)	2 (6.1)	2 (6.7)	0	0	3 (13.0)	0	7 (46.7)	9 (9.6)	4 (5.8)
≥5 cm	716 (31.5)	509 (29.6)	100 (38.0)	6 (18.2)	16 (53.3)	10 (52.6)	2 (66.7)	13 (56.5)	4 (80.0)	2 (13.3)	33 (35.1)	21 (30.4)
missing data	1321 (58.1)	1019 (59.2)	145 (55.1)	25 (75.8)	12 (40.0)	9 (47.4)	1 (33.3)	7 (30.4)	1 (20.0)	6 (40.0)	52 (55.3)	44 (63.8)
mitosis												
<5/50 HPF	352 (15.5)	252 (14.7)	38 (14.5)	11 (33.3)	7 (23.3)	3 (15.8)	0	6 (26.1)	2 (40.0)	5 (33.3)	18 (19.2)	10 (14.5)
≥5/50 HPF	445 (19.6)	332 (19.3)	63 (24.0)	4 (12.1)	6 (20.0)	5 (26.3)	1 (33.3)	7 (30.4)	2 (40.0)	3 (20.0)	14 (14.9)	8 (11.6)
missing data	1476 (64.9)	1135 (66.0)	162 (61.6)	18 (54.6)	17 (56.7)	11 (57.9)	2 (66.7)	10 (43.5)	1 (10.0)	7 (46.7)	62 (66.0)	51 (73.9)

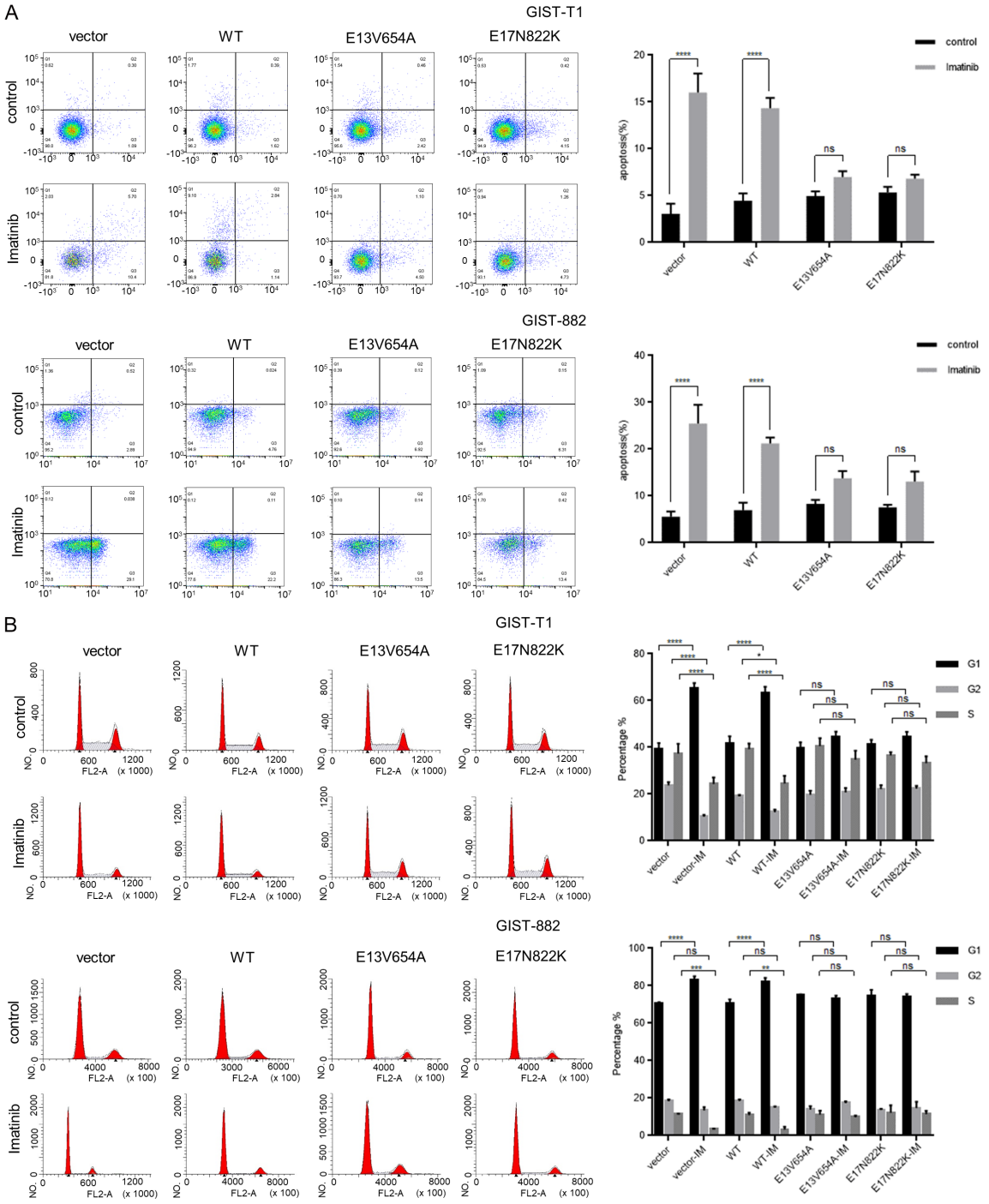

Supplementary Figure 1. Effect of Imatinib on apoptosis and cycle of GIST cells. A. Apoptosis analysis exhibited that Imatinib failed to induce apoptosis of GIST-T1 and GIST-882 cells expressing E13V654A and E17N822K forms of KIT. B. Cell cycle analysis showed that Imatinib's function in maintaining a higher proportion of G1 stage was impaired in GIST-T1 and GIST-882 cells expressing E13V654A or E17N822K forms of KIT.

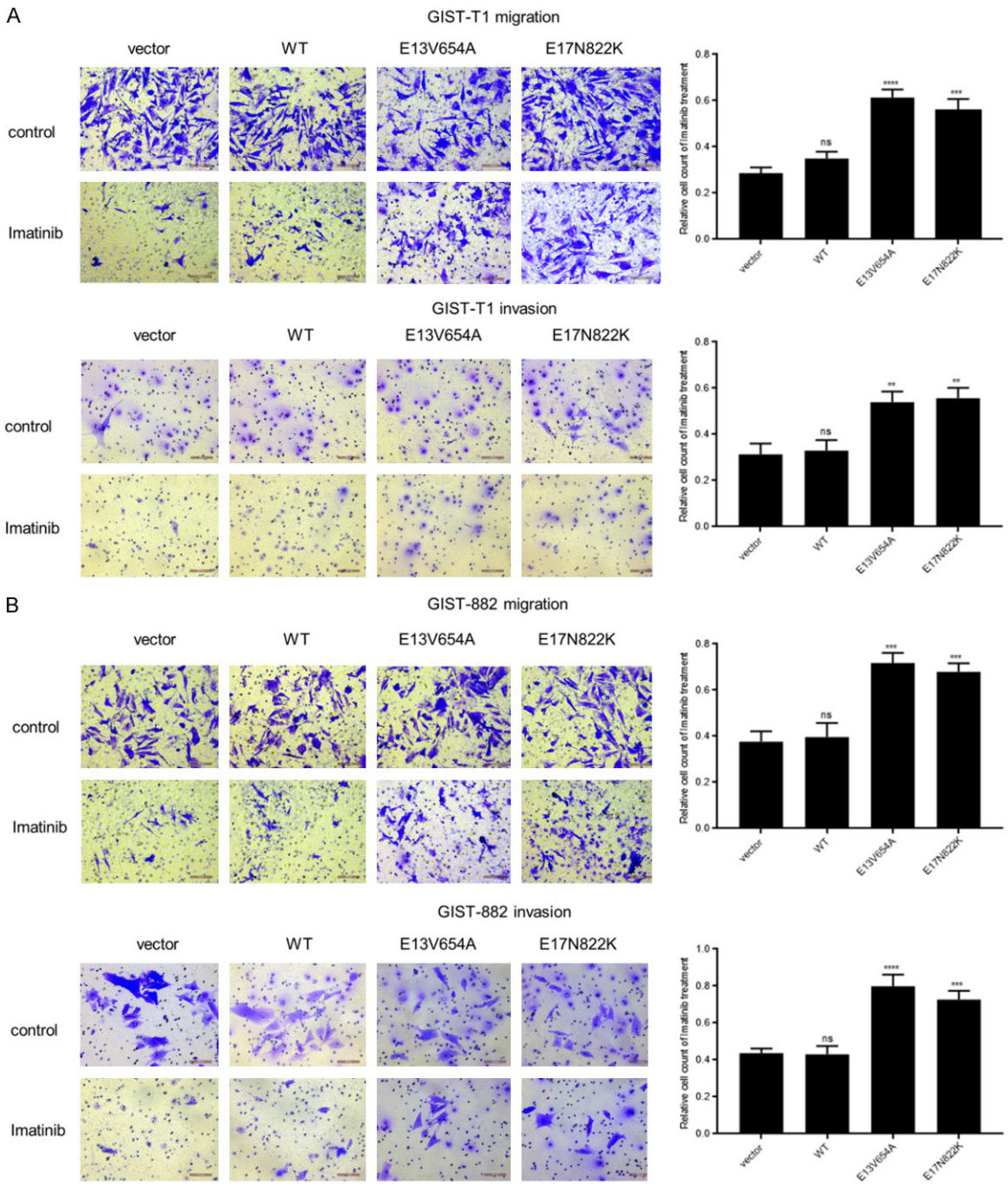

Supplementary Figure 2. Effects of Imatinib on migration and invasion of GIST cells. Transwell experiment revealed that Imatinib failed to remarkably decline migration and invasion cell number of GIST-T1 and GIST-882 cells expressing E13V654A and E17N822K forms of KIT.

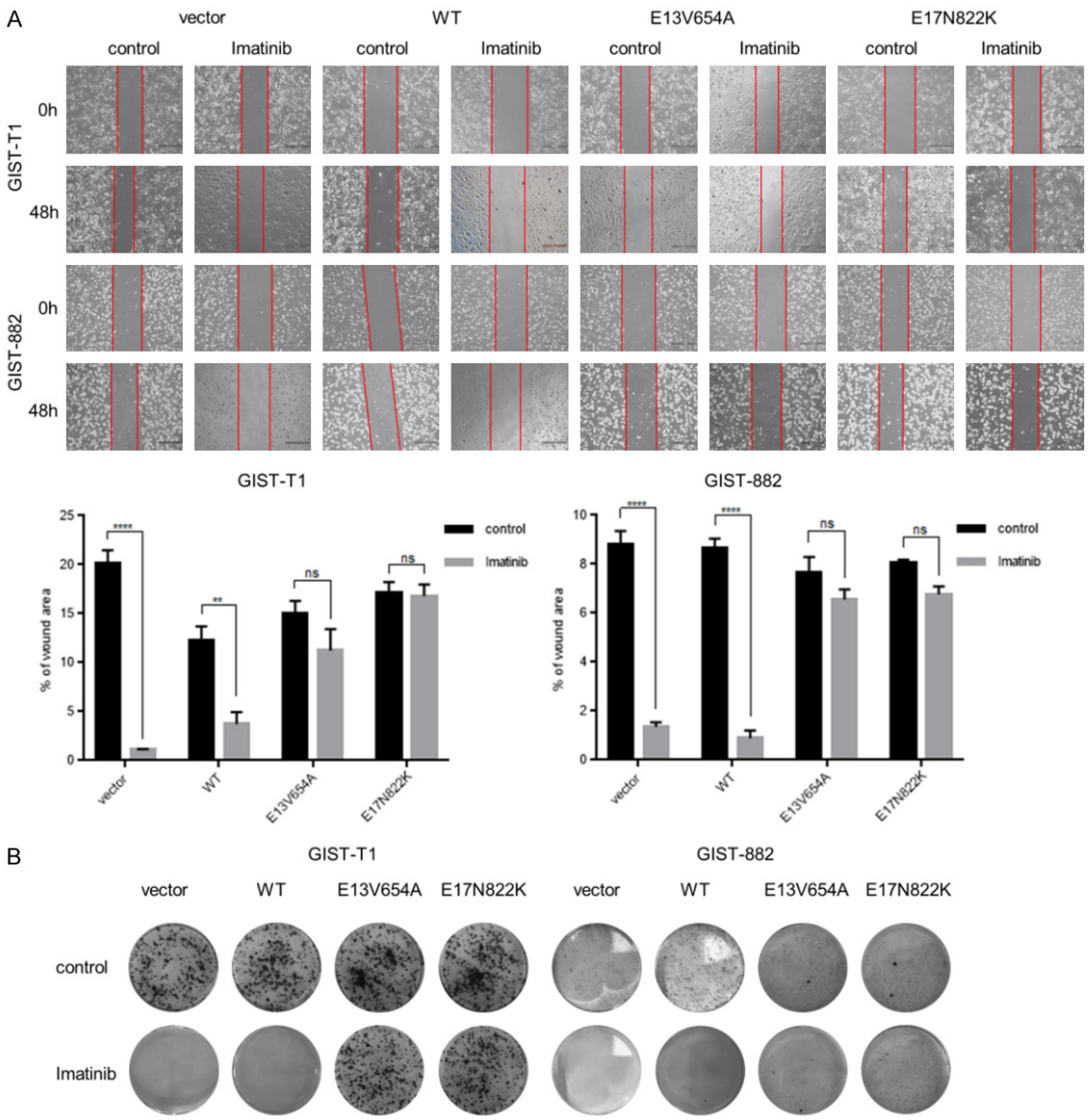

Supplementary Figure 3. Effect of Imatinib on wound-healing and plate clone formation of GIST Cells. A. Wound-healing assay showed that Imatinib failed to markedly inhibit crack of GIST-T1 and GIST-882 cells expressing E13V654A and E17N822K forms of KIT. B. Plate clone formation experiment exhibited that Imatinib failed to decrease colony number of GIST-T1 and GIST-882 cells expressing E13V654A and E17N822K forms of KIT.

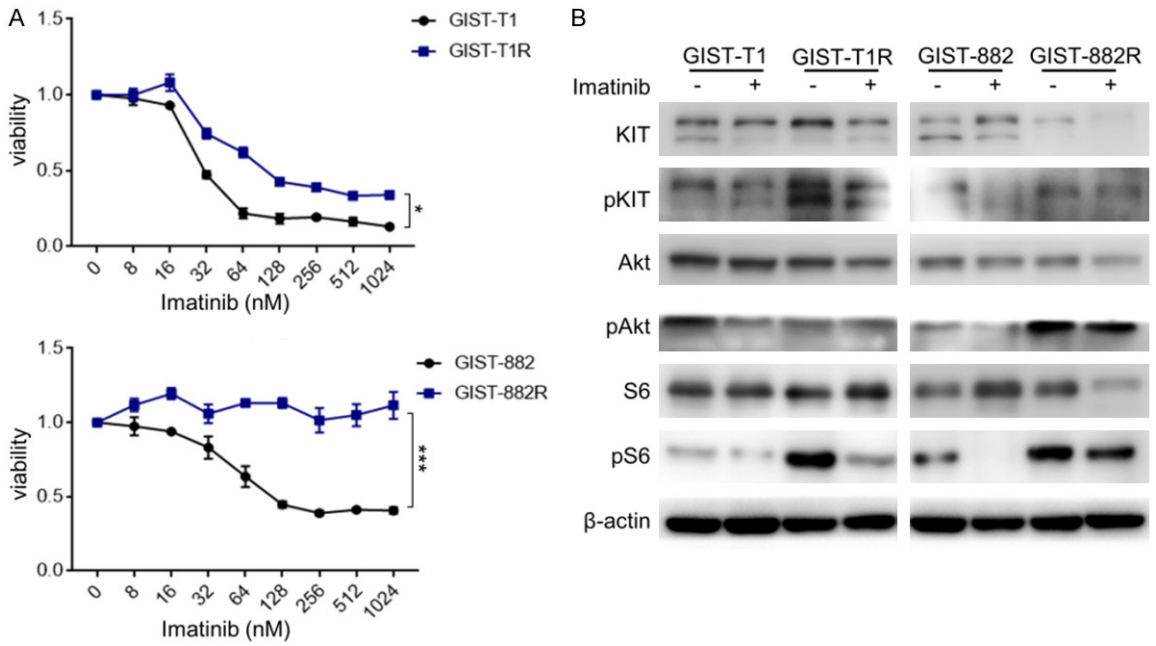

Supplementary Figure 4. Changes of viability and PI3K-Akt signaling in GIST cells with induced Imatinib-resistance. A. Viability curve of GIST-T1R and GIST-882R cells after 72 hours exposure to Imatinib. B. For groups with induced resistance and their progenitors, changes of KIT, p-KIT and the major components of the PI3K-Akt pathway were demonstrated after Imatinib treatment for 72 hours.

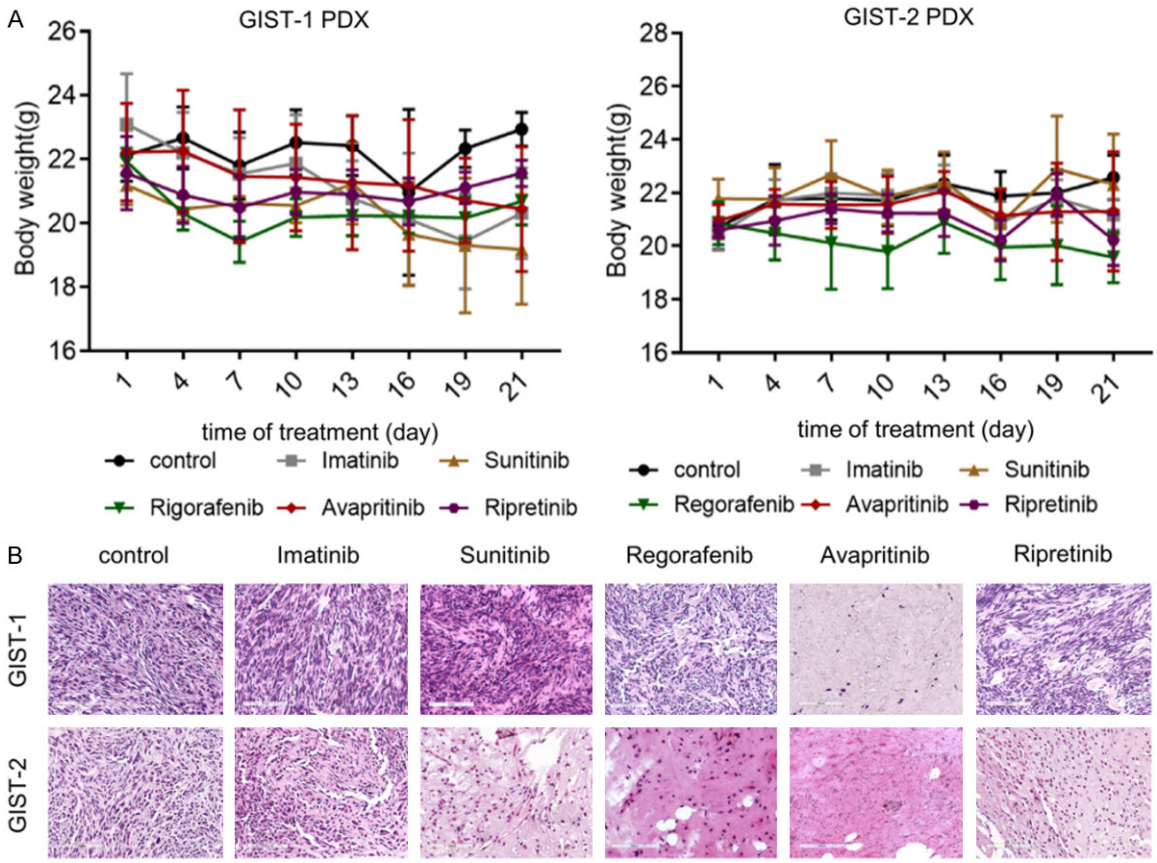

Supplementary Figure 5. Body weight of mice and histological characteristics of tumors after PDX tissue administration. A. Body weight of mice after 21 days exposure to Imatinib, Sunitinib, Regorafenib, Avapritinib and Ripretinib. B. Histological characteristics of tumors after PDX tissue administration.